Supplement of Atmos. Chem. Phys., 23, 14481–14503, 2023
https://doi.org/10.5194/acp-23-14481-2023-supplement

Atmospheric Chemistry and Physics
Open Access
EGU

Supplement of

Measurement Report: Investigation on the sources and formation processes of dicarboxylic acids and related species in urban aerosols before and during the COVID-19 lockdown in Jinan, East China

Jingjing Meng et al.

Correspondence to: Pingqing Fu (fupingqing@tju.edu.cn)

Supporting Information

Text S1. Stable carbon isotopic composition of diacids and related compounds

The isotopic analytical precision was ≤ 0.5‰ for a peak height (*m/z* 44) of 0.2 – 8 V. The isotopic composition of diacids and their derivatives is reported in the δ notation relative to the Pee Dee Belemnite (PDB) standard as follows:

$$\delta^{13}C\ (‰) = [(^{13}C/^{12}C)_{sample}/(^{13}C/^{12}C)_{PDB} - 1] \times 10^3$$

After the measurement of isotopic compositions of butyl esters, $\delta^{13}C$ of individual diacids is calculated by the following mass balance equation:

$$HOOC(CH_2)_nCOOH + 2C_4H_9OH \rightarrow H_9C_4OOC(CH_2)_nCOOC_4H_9 \quad (1)$$

(unknown $\delta^{13}C_{Diacid}$) (known $\delta^{13}C_{BuOH}$) (measured $\delta^{13}C_{DIBE}$)

$$\delta^{13}C_{DIBE} = f_{Diacid}\delta^{13}C_{Diacid} + f_{BuOH}\delta^{13}C_{BuOH} \quad (2)$$

where $\delta^{13}C_{Diacid}$, $\delta^{13}C_{BuOH}$, and $\delta^{13}C_{DIBE}$ represent the carbon isotopic composition of diacid, 1-butanol, and diacid dibutyl ester, respectively; f_{Diacid} and f_{BuOH} are fractions of carbon in the ester derived from diacid and butanol, respectively. f_{Diacid} and f_{BuOH} of C_2 are 0.2 and 0.8, respectively. The f_{Diacid} and f_{BuOH} values of other organic acids have been described in Kawamura and Watanabe (2004). Before actual sample analysis, we confirmed that $\delta^{13}C$ values of the working standards (a mixture of normal C_{16} – C_{30} alkanes with 0.55 – 2.83 ng μL^{-1}) were equivalent to the theoretical values within an analytical error of <0.2‰.

In addition, 2 µL internal standard (*n*-C_{13} alkane, -27.24 ‰) was spiked to the ester fraction, the esters were injected to a gas chromatograph interfaced to isotope ratio mass spectrometer to determine their stable carbon isotopic composition. GC was installed with a HP manual on-column injector and a capillary column (CIP-Sil 8CB, 60 m × 0.32 mm × 0.25 µm) was used with a column oven temperature programmed from 50 to 120°C at a rate of 30°C min^{-1} and then to 300°C at a rate of 6°C min^{-1}. Flow rate of carrier gas (He) was maintained at 1.7 mL min^{-1}.

In our manuscript, we stated that the recoveries of the target compounds were from 80% to 85%, which was not for yield during the derivatization reaction. The yield of derivatization reaction with 14% BF_3/*n*-butanol was 100%, during which the carboxyl functional group was fully derivatized to butyl ester, and the aldehyde and keto groups were fully derivatized to dibutoxy acetal. The $\delta^{13}C$ values for diacids and related compounds could not be directly determined, so these organic species are derivatized with BF_3/*n*-butanol to dibutyl esters which are analyzed for the stable carbon isotopic composition using a GC-IR-MS. The $\delta^{13}C$ values for individual diacids are then calculated from $\delta^{13}C$ of 1-butanol and butyl ester derivative using a mass balance equation. The accuracy of the $\delta^{13}C$ measurement for these target compounds is within 0.8‰. The method developed for the determination of stable carbon isotopic composition of diacids and related compounds isolated from aerosols is reliable and scientific, and has been used widely in many studies (Aggarwal and Kawamura, 2008; Meng et al., 2020; Mkoma et al., 2014; Pavuluri et al., 2011; Qi et al., 2022; Shen et al., 2022; Shen et al., 2023; Wang et al., 2012; Wang and Kawamura, 2006; Xu et al., 2022a; Xu et al., 2022b; Zhang et al., 2016; Zhao et al., 2018).

Text S2. Potential source contribution function

To analyze air masses from different origins reaching the sampling site, 48 h backward trajectory was performed using a Hybrid Single Particle Lagrangian Integrated Trajectory (HYSPLIT4) model. To determine the potential source regions of total diacids and related compounds, the potential source contribution function (PSCF) was used and detailed information was described in our previous study (Li et al., 2021).

Text S3. Positive Matrix Factorization (PMF) model

In this study, the Environmental Protection Agency (EPA) PMF version 5.0 was used to perform the analysis (Norris et al., 2014). The PMF model has been widely applied to obtain source apportionment of organic aerosols in $PM_{2.5}$. It decomposes the sample data matrix into factor contribution matrix and factor outline matrix, and then the source types and their contribution are calculated based on the input data. The PMF model is described as follows:

$$X_{ij} = \sum_{k=1}^{P} g_{ik} f_{ki} + e_{ij} \quad (3)$$

where X_{ij} represents the concentration of the species j detected in the sample i, p represents the number of contribution factors of the samples, g_{ik} represents the relative contribution of factor k to the sample i, f_{kj} represents the mass contribution of the species j in the factor k, e_{ij} represents the error of the species j measured in the sample i. The matrix x is continuously decomposed to get minimum values of Q in order to obtain the optimal matrices g and f. The Q is defined as follows:

$$Q = \sum_{i=1}^{n}\sum_{j=1}^{m}\left(\frac{x_{ij} - \sum_{k=1}^{P} g_{ik} f_{ki}}{u_{ij}}\right) = \sum_{i=1}^{n}\sum_{j=1}^{m}\left(\frac{e_{ij}}{u_{ij}}\right)^2 \quad (4)$$

where u_{ij} is the uncertainty of the concentration of the species j in the sample i. If the measured species concentration is below the method detection limit (MDL), it is replaced by 1/2 MDL, and the corresponding uncertainty is 5/6 MDL. When the concentration is higher than the MDL, the uncertainty is calculated as follows:

$$\text{Uncertainty} = \sqrt{(error\ fraction * concentration)^2 + (0.5 * MDL)^2} \quad (5)$$

where the error fraction is the estimation of the analytical uncertainty of the measured concentration or flux (Hovorka et al., 2015; Shrivastava et al., 2007; Wu et al., 2020).

Based on Norris et al. (2004) and Nayebare et al. (2018), the comparatively high signal-to-noise (S/N) ratios > 5 could be labeled as "strong" to enhance their effect on the model results for all species. The S/N ratios of species used in PMF model were higher than 8, thus these species were labeled as "strong".

The concentrations of selected major diacids (including C_2, C_3, C_4, C_9, and Ph), oxoacids (including Pyr and ωC_2), and α-dicarbonyls used in the PMF model accounted for 76.1 ± 6.0% and 82.8 ± 6.6% of total concentration of detected organic components (TDOCs) before and during the LCD, respectively. The other organic compounds (including C_5-C_8, C_{10}, C_{11}, iC_4-iC_6, M, F, mM, iPh, tPh, kC_3, kC_7, ωC_3, ωC_4 and ωC_7-ωC_9) presented relatively low concentrations and occasionally were below the detection limit, which could enhance the uncertainties. Moreover, these unconsidered organic compounds were less indicative for identified sources than the selected major acids. Thus, we kept those organic compounds with low concentrations out of the model.

As discussed in Section 3.3, SO_4^{2-} and LWC could be considered as significant influencing factors during the aqueous formation of C_2 before the LCD, and O_3 was a key influencing factor during the photochemical formation of C_2 during the

LCD. Therefore, those species have been put in the PMF model to distinguish the aqueous pathway from the gaseous photochemical pathway of the diacids formation.

The PMF model provides three uncertainty estimation methods to examine the robustness of the solution, namely, bootstrap (BS), displacement (DISP), and bootstrap combined displacement (BS-DISP), which can also provide a distribution range of the factor profiles through resampling for multi times and displacing with the Q value change within the preset value. Further details related to the error estimation methods can refer to Brown et al. (2015), Vossler et al. (2016), and Wang et al. (2018). In this study, PMF solutions of 4-6 factors were analyzed and showed the convergence result. The relevant Q values and Q_{true}/Q_{robust} for these solutions were shown in Table S5. Finally, the five-factor solution was selected as the best solution with physical means before (Q_{true}/Q_{robust}=1.05, $Q_{true}/Q_{expected}$=1.27) and during the LCD (Q_{true}/Q_{robust}=1.05, $Q_{true}/Q_{expected}$=1.36), respectively. The error code of DISP before or during the LCD was 0 (Table S6), indicating no error. The values in the first row of dQ^{max} = 4 were zero before and during the LCD (Table S6), indicating that there was no significant rotational ambiguity and that the solution was sufficiently robust to be used. Mapping over 82% of the factors before or during the LCD indicated that the BS uncertainties could be interpreted and the number of factors may be appropriate. The Largest decrease in Q before and during the LCD was -0.048% and -0.061%, respectively (Table S6), suggesting the five-factor solution was more reliably attributed to sources than the four-factor solution and six-factor solution.

Text S4. Quality assurance/quality control (QA/QC) of online air quality data

Those measured parameters were obtained from one of the State Controlling Air Sampling Sites in Jinan (https://www.aqistudy.cn/). The QA/QC was operated strictly by professionals followed by “Technical Specification for Automatic Monitoring of Ambient Air Quality”, “Technical Standard for Ambient Air Quality Monitoring”, and “Technical Instruction” formulated by the Ministry of Ecology and Environment of the People's Republic of China.

Text S5. Aqueous phase formation of SO_4^{2-} before the LCD

The aqueous phase conversion of dissolved SO_2 to SO_4^{2-} is probably the most important chemical formation pathway in the North China Plain during the wintertime (Sun et al., 2013; Wang et al., 2014; Zhang et al., 2015). A few studies have demonstrated that LWC and RH are considered as key factors determining SO_4^{2-} formation via aqueous reactions (Bikkina et al., 2017; Cheng et al., 2016). We observed a robust relationship of SO_4^{2-} with RH (R^2 = 0.58) and LWC (R^2 = 0.71) before the LCD (Fig. S3), indicating that the aqueous oxidation determined by LWC and RH played a dominant role in the formation of SO_4^{2-} before the LCD.

Table S1. Correlation coefficients (R^2, $P < 0.01$) of levoglucosan and K^+ with EC, OC, WSOC, C_2, C_9, diacids, and total detected organic components (TDOCs).

	EC	OC	WSOC	K^+	C_2	C_9	Diacids	TDOCs
Before the LCD								
Levoglucosan	0.62	0.66	0.45	0.77	0.61	0.74	0.62	0.73
K^+	0.57	0.56	0.55	1.00	0.68	0.64	0.59	0.65
During the LCD								
Levoglucosan	0.15	0.09	0.05	0.86	0.02	0.06	0.02	0.03
K^+	0.10	0.08	0.02	1.00	0.03	0.02	0.11	0.13

Table S2. Statistic test for the differences in concentrations and mass ratios of major species in $PM_{2.5}$ before and during the LCD in Jinan.

Species/ Ratios	*p*
$PM_{2.5}$	**0.000**[a]
PM_{10}	**0.000**[a]
CO	**0.000**[a]
SO_2	**0.000**[a]
NOx	**0.000**[a]
O_3	**0.000**[a]
RH (Relative humidity)	**0.000**[a]
Wind speed	**0.000**[a]
OC (Organic carbon)	**0.000**[a]
EC (Elemental carbon)	**0.000**[a]
WSOC (Water-soluble organic compounds)	0.098[b]
SIA (Total concentration of SO_4^{2-}, NO_3^-, and NH_4^+)	**0.001**[a]
LWC (Liquid water content)	**0.000**[a]
pH_{is} (Particle in-situ pH)	0.256[b]
C_2 (Oxalic acid)	**0.004**[b]
C_9 (Azelaic acid)	**0.000**[a]
Ph (Phthalic acid)	**0.026**[b]
Diacids (Dicarboxylic acids)	**0.018**[b]
Oxoacids	**0.003**[a]
α-Dicarbonyls	0.881[b]
TDOCs (Total detected organic components)	**0.014**[a]
Levoglucosan	**0.003**[a]
C_2/Diacids	**0.000**[a]
C_2/TDOCs	**0.005**[a]
C_2/C_4 (Succinic acid)	**0.000**[a]
C_3 (Malonic acid)/C_4	**0.000**[a]
C_9 (Azelaic acid)/Diacids	**0.000**[a]
Ph/Diacids	**0.027**[a]

[a]When the variables follow a normal distribution, ANOVA was employed to analyze the statistically significant differences between these two datasets before and during the LCD. [b]Otherwise, the Kruskal-Wallis test was used. Bold font represented the species (or ratios) that were statistically significantly different ($p < 0.05$).

Table S3. Statistic test for the day-night differences in concentrations and mass ratios of major species in $PM_{2.5}$ before or during the LCD, respectively.

Species/ Ratios	Before the LCD	During the LCD
	p	*p*
C_2	**0.011**[a]	**0.042**[a]
Diacids	**0.032**[a]	**0.046**[b]
C_2/Diacids	**0.018**[a]	**0.041**[b]
C_2/TDOCs	**0.017**[b]	**0.029**[a]
Na^+	0.764[b]	0.362[b]
Ca^{2+}	0.443[b]	0.637[b]
Mg^{2+}	1.000[b]	0.784[b]
C_2/Levoglucosan	**0.037**[a]	0.074[b]
C_2/K^+	**0.000**[a]	0.081[b]

[a]When the variables follow a normal distribution, ANOVA was employed to analyze the statistically significant differences during the daytime and nighttime. [b]Otherwise, the Kruskal-Wallis test was used. Bold font represented the species (or ratios) that were statistically significantly different ($p < 0.05$).

Table S4. Comparison of C_2, diacids, and TDOCs concentrations (ng m^{-3}), and C_3/C_4 ratio in Jinan with those in other Asian megacities during the wintertime.

Location	Period	Size	C_2	Diacids	TDOCs	C_2/C_4	C_3/C_4	Data source
14 Chinese cities	13–14 Jan 2003	$PM_{2.5}$	558±351	904±480	974±499	7.0	0.5	(Ho et al., 2007)
Beijing, China	Dec 2013	$PM_{2.5}$	149±123	366±261	450±368	4.7	0.6±0.1	(Zhao et al., 2018)
Chengdu, China	7–23 Jan 2013	$PM_{2.1}$	1380	3390	4285	3.2	0.5±0.1	(Li et al., 2015)
Xi'an, China	Jan–Feb 2009	PM_{10}	1162±570	1843±810	2207±1044	11.9	1.0	(Cheng et al., 2013)
Tianjin, China	23 Nov–11 Dec 2016	$PM_{2.1}$	526±335	1223±623	1438±739	3.2	0.3	(Devineni et al., 2023)
Liaocheng, China	17 Jan–16 Feb 2016	$PM_{2.5}$	817±544	1415±899	1677±1026	3.6±0.9	0.4±0.2	(Meng et al., 2020)
Guangzhou, China	Dec 2006–Jan 2007	$PM_{2.5}$	182±106	384±171	414±184	9.9	0.7	(Ho et al., 2011)
Tianjin, China	1–28 Feb 2019	$PM_{2.5}$	668±470	1137±707	1561	7.6	1.0	(Zhao et al., 2023)
Padori, South Korea	1–28 Feb 2019	$PM_{2.5}$	389±204	582±266	750	8.3	0.7	(Zhao et al., 2023)
Daejeon, South Korea	1–28 Feb 2019	$PM_{2.5}$	516±327	784±446	1108	10.0	0.7	(Zhao et al., 2023)
Ulaanbaatar, Mongolia	Nov 2007–Jan 2008	$PM_{2.5}$	107±28	536±156	697±207	1.8±0.8	0.2±0.1	(Jung et al., 2010)
Chennai, India	23–28 Jan 2007	PM_{10}	472±137	695 ± 176	765	11.8	1.5	(Pavuluri et al., 2010)
Chennai, India	29 Jan–6 Feb 2007	PM_{10}	380±89	641 ± 157	719	7.9	1.2	(Pavuluri et al., 2010)
Tokyo, Japan	20–21 November 1989	TSP	186	438	595	3.9	0.9	(Kawamura and Yasui, 2005)
Jinan, China	6–23 Jan 2020	$PM_{2.5}$	181±48	351±92	437±117	3.9±1.5	0.3±0.1	This study
Jinan, China	31 Jan–17 Feb 2020	$PM_{2.5}$	239±108	386±127	486±144	8.4±3.4	1.6±0.4	This study

115

Table S5. Q values for PMF Analysis with different number of factors.

Number of factors	*R^2 for all input species	Q_{true}	Q_{robust}	$Q_{true}/Q_{expected}$	Q_{true}/Q_{robust}
(a) Before the LCD					
4	0.63-0.98	1556.1	1480.2	2.241	1.051
5	0.68-0.99	1176.9	1123.5	1.273	1.047
6	0.60-0.98	905.2	851.6	2.454	1.062
(a) During the LCD					
4	0.32-0.96	2722.0	2396.5	2.624	1.136
5	0.52-0.99	1859.3	1768.2	1.360	1.052
6	0.37-0.84	1334.1	1294.6	2.912	1.071

*R^2 between the measured and predicted species

Table S6. Summary of error estimation diagnostics from BS and DISP for PMF (a) Before the LCD and (b) During the LCD.

(a) Before the LCD

DISP Diagnostics		Error code: 0		Largest decrease in Q:-0.048		
Factor Swaps	dQ^{max}=4	0	0	0	0	0
	dQ^{max}=8	0	0	0	1	1
	dQ^{max}=15	0	1	3	6	0
	dQ^{max}=25	0	1	5	8	10

(b) During the LCD

DISP Diagnostics		Error code: 0		Largest decrease in Q:-0.061		
Factor Swaps	dQ^{max}=4	0	0	0	0	0
	dQ^{max}=8	0	0	0	0	0
	dQ^{max}=15	0	0	1	1	0
	dQ^{max}=25	0	1	8	10	6

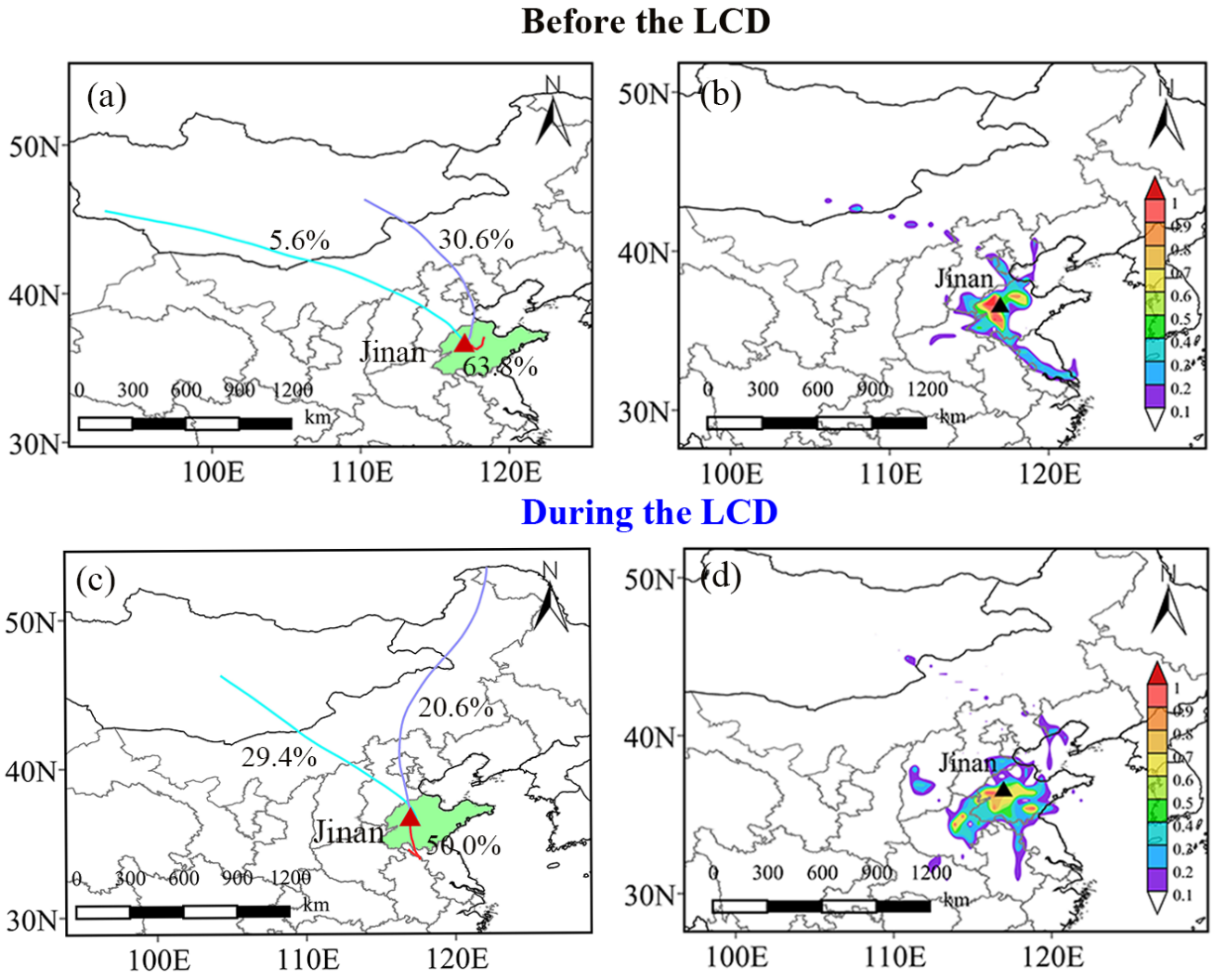

125 **Figure S1. 48-h backward trajectories of air masses arriving at Jinan (a) before the LCD and (b) during the LCD. Potential source contribution function (PSCF) analysis of total detected organic compounds (TDOCs) in $PM_{2.5}$ (c) before the LCD and (d) during the LCD.**

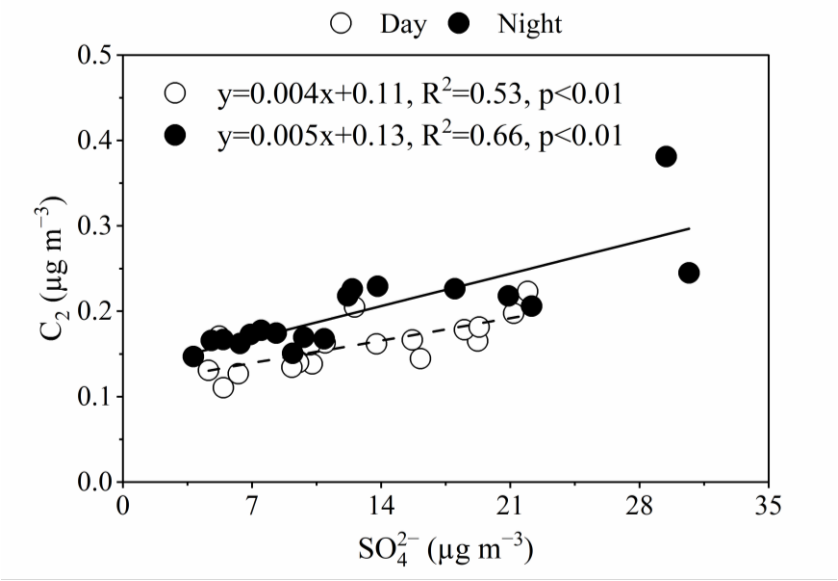

Figure S2. Correlation analysis for C_2 and SO_4^{2-} during the daytime and nighttime before the LCD.

130

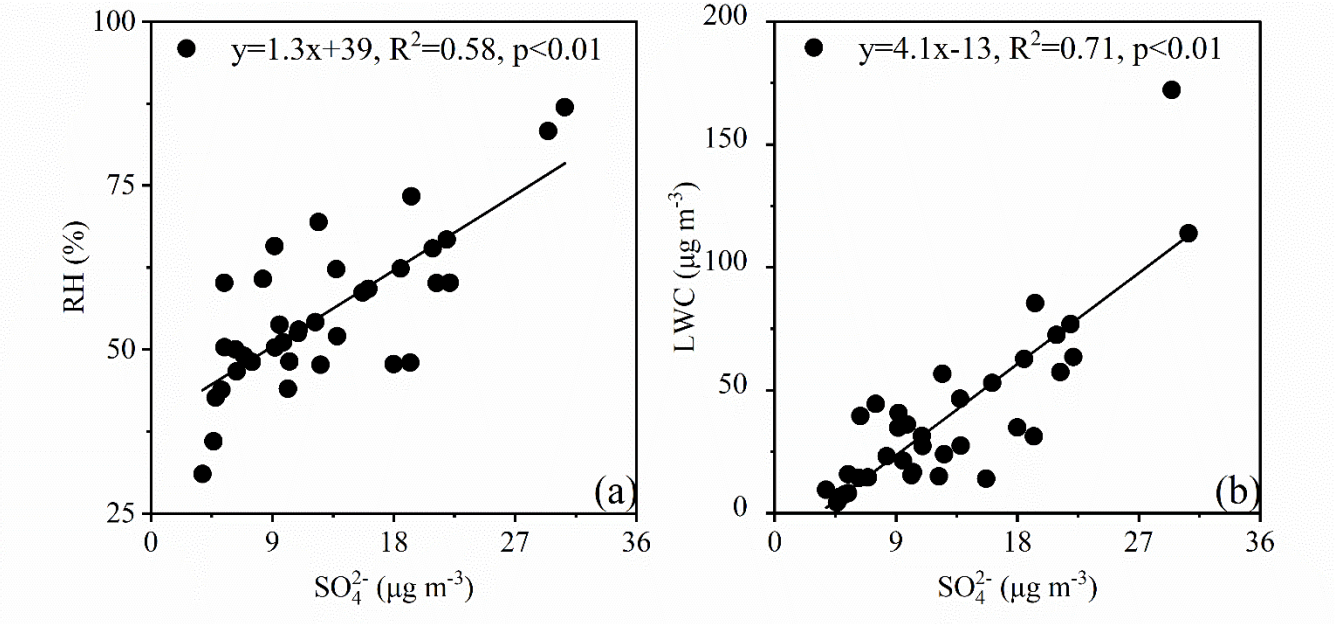

Figure S3. Relationships of SO_4^{2-} with (a) RH and (b) LWC before the LCD.

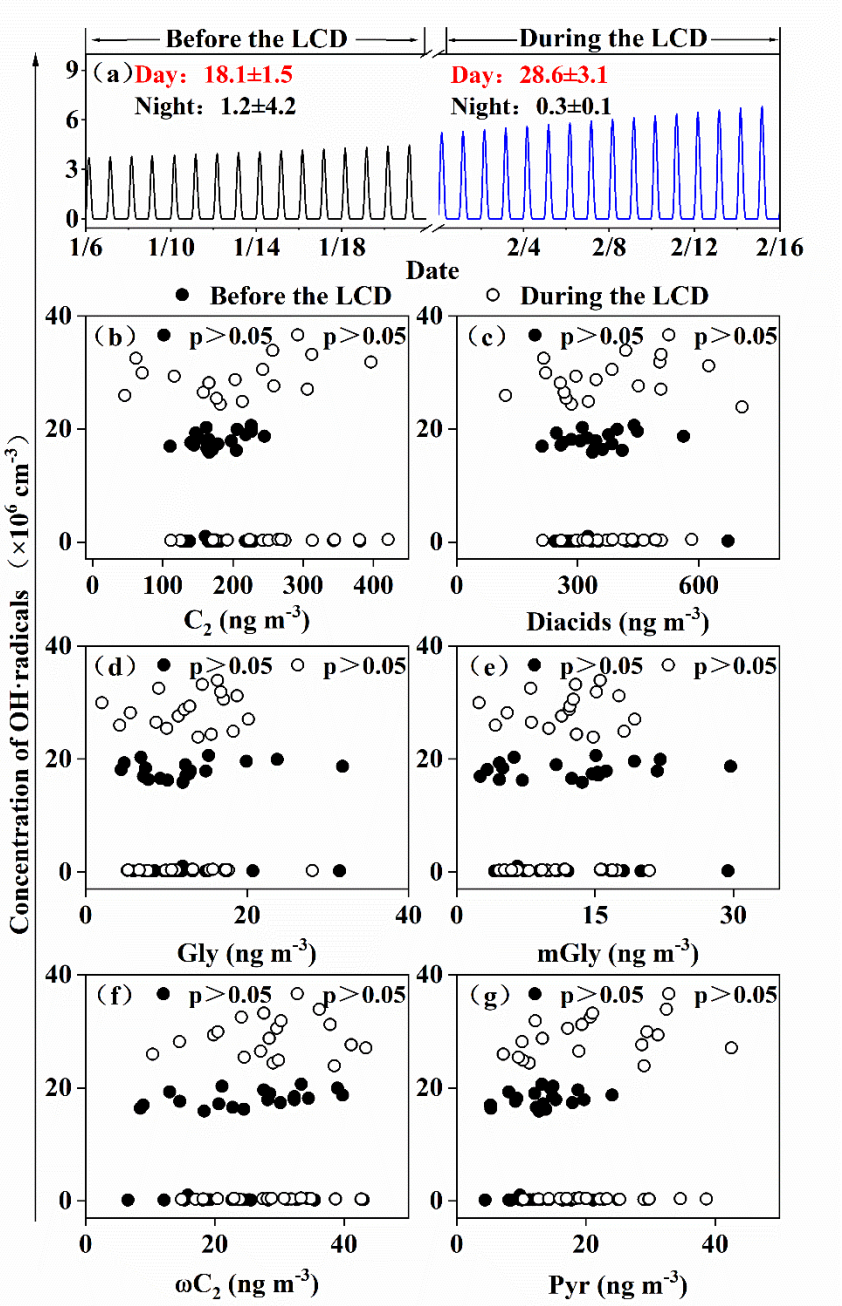

135 **Figure S4. (a) Time series of OH· radical concentration per hour, and correlations of OH· radicals with (b) C_2, (c) Diacids, (d) Gly, (e) mGly, (f) ωC_2, and (g) Pyr before and during the LCD.**

References

Aggarwal, S. G. and Kawamura, K.: Molecular distributions and stable carbon isotopic compositions of dicarboxylic acids and related compounds in aerosols from Sapporo, Japan: Implications for photochemical aging during long-range atmospheric transport, Journal of Geophysical Research: Atmospheres, 113, D14301, 10.1029/2007jd009365, 2008.

Bikkina, S., Kawamura, K., and Sarin, M.: Secondary Organic Aerosol Formation over Coastal Ocean: Inferences from Atmospheric Water-Soluble Low Molecular Weight Organic Compounds, Environmental Science & Technology, 51, 4347-4357, 10.1021/acs.est.6b05986, 2017.

Brown, S. G., Eberly, S., Paatero, P., and Norris, G. A.: Methods for estimating uncertainty in PMF solutions: Examples with ambient air and water quality data and guidance on reporting PMF results, Science of The Total Environment, 518-519, 626-635, https://doi.org/10.1016/j.scitotenv.2015.01.022, 2015.

Cheng, C., Wang, G., Zhou, B., Meng, J., Li, J., Cao, J., and Xiao, S.: Comparison of dicarboxylic acids and related compounds in aerosol samples collected in Xi'an, China during haze and clean periods, Atmospheric Environment, 81, 443-449, http://dx.doi.org/10.1016/j.atmosenv.2013.09.013, 2013.

Cheng, Y., Zheng, G., Wei, C., Mu, Q., Zheng, B., Wang, Z., Gao, M., Zhang, Q., He, K., Carmichael, G., Pöschl, U., and Su, H.: Reactive nitrogen chemistry in aerosol water as a source of sulfate during haze events in China, Science Advances, 2, 2016.

Devineni, S. R., Pavuluri, C. M., Wang, S., Ren, L., Xu, Z., Li, P., Fu, P., and Liu, C.-Q.: Size-Resolved Characteristics and Sources of Inorganic Ions, Carbonaceous Components and Dicarboxylic Acids, Benzoic Acid, Oxocarboxylic Acids and α-Dicarbonyls in Wintertime Aerosols from Tianjin, North China, Aerosol Science and Engineering, 7, 1-22, 10.1007/s41810-022-00159-0, 2023.

Ho, K. F., Cao, J. J., Lee, S. C., Kawamura, K., Zhang, R. J., Chow, J. C., and Watson, J. G.: Dicarboxylic acids, ketocarboxylic acids, and dicarbonyls in the urban atmosphere of China, Journal of Geophysical Research: Atmospheres, 112, D22S27, 10.1029/2006jd008011, 2007.

Ho, K. F., Ho, S. S. H., Lee, S. C., Kawamura, K., Zou, S. C., Cao, J. J., and Xu, H. M.: Summer and winter variations of dicarboxylic acids, fatty acids and benzoic acid in PM_{2.5} in Pearl Delta River Region, China, Atmos. Chem. Phys., 11, 2197-2208, 10.5194/acp-11-2197-2011, 2011.

Hovorka, J., Pokorná, P., Hopke, P. K., Křůmal, K., Mikuška, P., and Píšová, M.: Wood combustion, a dominant source of winter aerosol in residential district in proximity to a large automobile factory in Central Europe, Atmospheric Environment, 113, 98-107, https://doi.org/10.1016/j.atmosenv.2015.04.068, 2015.

Jung, J., Tsatsral, B., Kim, Y. J., and Kawamura, K.: Organic and inorganic aerosol compositions in Ulaanbaatar, Mongolia, during the cold winter of 2007 to 2008: Dicarboxylic acids, ketocarboxylic acids, and α-dicarbonyls, Journal of Geophysical Research: Atmospheres, 115, D22203, 10.1029/2010jd014339, 2010.

Kawamura, K. and Watanabe, T.: Determination of Stable Carbon Isotopic Compositions of Low Molecular Weight

Dicarboxylic Acids and Ketocarboxylic Acids in Atmospheric Aerosol and Snow Samples, Anal. Chem., 76, 5762-5768, 10.1021/ac049491m, 2004.

Kawamura, K. and Yasui, O.: Diurnal changes in the distribution of dicarboxylic acids, ketocarboxylic acids and dicarbonyls in the urban Tokyo atmosphere, Atmospheric Environment, 39, 1945-1960, http://dx.doi.org/10.1016/j.atmosenv.2004.12.014, 2005.

Li, X., Yang, Z., Fu, P., Yu, J., Lang, Y., Liu, D., Ono, K., and Kawamura, K.: High abundances of dicarboxylic acids, oxocarboxylic acids, and α-dicarbonyls in fine aerosols (PM2.5) in Chengdu, China during wintertime haze pollution, Environmental Science and Pollution Research, 22, 12902-12918, 10.1007/s11356-015-4548-x, 2015.

Li, Z., Zhou, R., Wang, Y., Wang, G., Chen, M., Li, Y., Wang, Y., Yi, Y., Hou, Z., Guo, Q., and Meng, J.: Characteristics and sources of amine-containing particles in the urban atmosphere of Liaocheng, a seriously polluted city in North China during the COVID-19 outbreak, Environmental Pollution, 289, 117887, https://doi.org/10.1016/j.envpol.2021.117887, 2021.

Meng, J., Liu, X., Hou, Z., Yi, Y., Yan, L., Li, Z., Cao, J., Li, J., and Wang, G.: Molecular characteristics and stable carbon isotope compositions of dicarboxylic acids and related compounds in the urban atmosphere of the North China Plain: Implications for aqueous phase formation of SOA during the haze periods, Science of The Total Environment, 705, 135256, https://doi.org/10.1016/j.scitotenv.2019.135256, 2020.

Mkoma, S. L., Kawamura, K., and Tachibana, E.: Stable carbon isotopic compositions of low-molecular-weight dicarboxylic acids, glyoxylic acid and glyoxal in tropical aerosols: implications for photochemical processes of organic aerosols, Tellus B: Chemical and Physical Meteorology, 66, 23702, 10.3402/tellusb.v66.23702, 2014.

Nayebare, S. R., Aburizaiza, O. S., Siddique, A., Carpenter, D. O., Hussain, M. M., Zeb, J., Aburiziza, A. J., and Khwaja, H. A.: Ambient air quality in the holy city of Makkah: A source apportionment with elemental enrichment factors (EFs) and factor analysis (PMF), Environmental Pollution, 243, 1791-1801, https://doi.org/10.1016/j.envpol.2018.09.086, 2018.

Norris, G., Duvall, R., Brown, S., & Bai, S. EPA positive matrix factorization (PMF) 5.0 fundamentals and user guide prepared for the US Environmental Protection Agency Office of Research and Development, Washington, DC, 2004.

Pavuluri, C. M., Kawamura, K., Swaminathan, T., and Tachibana, E.: Stable carbon isotopic compositions of total carbon, dicarboxylic acids and glyoxylic acid in the tropical Indian aerosols: Implications for sources and photochemical processing of organic aerosols, Journal of Geophysical Research: Atmospheres, 116, https://doi.org/10.1029/2011JD015617, 2011.

Pavuluri, C. M., Kawamura, K., Tachibana, E., and Swaminathan, T.: Elevated nitrogen isotope ratios of tropical Indian aerosols from Chennai: Implication for the origins of aerosol nitrogen in South and Southeast Asia, Atmospheric Environment, 44, 3597-3604, https://doi.org/10.1016/j.atmosenv.2010.05.039, 2010.

Qi, W., Wang, G., Dai, W., Liu, S., Zhang, T., Wu, C., Li, J., Shen, M., Guo, X., Meng, J., and Li, J.: Molecular characteristics

and stable carbon isotope compositions of dicarboxylic acids and related compounds in wintertime aerosols of Northwest China, Scientific Reports, 12, 11266, 10.1038/s41598-022-15222-6, 2022.

Shen, M., Ho, K. F., Dai, W., Liu, S., Zhang, T., Wang, Q., Meng, J., Chow, J. C., Watson, J. G., Cao, J., and Li, J.: Distribution and stable carbon isotopic composition of dicarboxylic acids, ketocarboxylic acids and α-dicarbonyls in fresh and aged biomass burning aerosols, Atmos. Chem. Phys., 22, 7489-7504, 10.5194/acp-22-7489-2022, 2022.

Shen, M., Qi, W., Guo, X., Dai, W., Wang, Q., Liu, Y., Zhang, Y., Cao, Y., Chen, Y., Li, L., Liu, H., Cao, J., and Li, J.: Influence of vertical transport on chemical evolution of dicarboxylic acids and related secondary organic aerosol from surface emission to the top of Mount Hua, Northwest China, Science of The Total Environment, 858, 159892, https://doi.org/10.1016/j.scitotenv.2022.159892, 2023.

Shrivastava, M. K., Subramanian, R., Rogge, W. F., and Robinson, A. L.: Sources of organic aerosol: Positive matrix factorization of molecular marker data and comparison of results from different source apportionment models, Atmospheric Environment, 41, 9353-9369, https://doi.org/10.1016/j.atmosenv.2007.09.016, 2007.

Vossler, T., Černikovský, L., Novák, J., and Williams, R.: Source apportionment with uncertainty estimates of fine particulate matter in Ostrava, Czech Republic using Positive Matrix Factorization, Atmospheric Pollution Research, 7, 503-512, https://doi.org/10.1016/j.apr.2015.12.004, 2016.Bikkina, S., Kawamura, K., and Sarin, M.: Secondary Organic Aerosol Formation over Coastal Ocean: Inferences from Atmospheric Water-Soluble Low Molecular Weight Organic Compounds, Environmental Science & Technology, 51, 4347-4357, 10.1021/acs.est.6b05986, 2017.

Sun, Y. L., Wang, Z. F., Fu, P. Q., Yang, T., Jiang, Q., Dong, H. B., Li, J., and Jia, J. J.: Aerosol composition, sources and processes during wintertime in Beijing, China, Atmos. Chem. Phys., 13, 4577-4592, 10.5194/acp-13-4577-2013, 2013.

Wang, G., Kawamura, K., Cheng, C., Li, J., Cao, J., Zhang, R., Zhang, T., Liu, S., and Zhao, Z.: Molecular Distribution and Stable Carbon Isotopic Composition of Dicarboxylic Acids, Ketocarboxylic Acids, and α-Dicarbonyls in Size-Resolved Atmospheric Particles From Xi'an City, China, Environmental Science & Technology, 46, 4783-4791, 10.1021/es204322c, 2012.

Wang, H. and Kawamura, K.: Stable carbon isotopic composition of low-molecular-weight dicarboxylic acids and ketoacids in remote marine aerosols, Journal of Geophysical Research: Atmospheres, 111, https://doi.org/10.1029/2005JD006466, 2006.

Wang, Y., Zhang, Q., Jiang, J., Zhou, W., Wang, B., He, K., Duan, F., Zhang, Q., Philip, S., and Xie, Y.: Enhanced sulfate formation during China's severe winter haze episode in January 2013 missing from current models, Journal of Geophysical Research: Atmospheres, 119, 10,425-410,440, https://doi.org/10.1002/2013JD021426, 2014.

Wu, X., Cao, F., Haque, M., Fan, M.-Y., Zhang, S.-C., and Zhang, Y.-L.: Molecular composition and source apportionment of fine organic aerosols in Northeast China, Atmospheric Environment, 239, 117722, https://doi.org/10.1016/j.atmosenv.2020.117722, 2020.

Xu, B., Tang, J., Tang, T., Zhao, S., Zhong, G., Zhu, S., Li, J., and Zhang, G.: Fates of secondary organic aerosols in the

atmosphere identified from compound-specific dual-carbon isotope analysis of oxalic acid, Atmos. Chem. Phys. Discuss., 2022, 1-32, 10.5194/acp-2022-707, 2022a.

Xu, B., Zhang, G., Gustafsson, Ö., Kawamura, K., Li, J., Andersson, A., Bikkina, S., Kunwar, B., Pokhrel, A., Zhong, G., Zhao, S., Li, J., Huang, C., Cheng, Z., Zhu, S., Peng, P., and Sheng, G.: Large contribution of fossil-derived components to aqueous secondary organic aerosols in China, Nature Communications, 13, 5115, 10.1038/s41467-022-32863-3, 2022b.

Zhang, R., Wang, G., Guo, S., Zamora, M. L., Ying, Q., Lin, Y., Wang, W., Hu, M., and Wang, Y.: Formation of Urban Fine Particulate Matter, Chemical Reviews, 115, 3803-3855, 10.1021/acs.chemrev.5b00067, 2015.

Zhang, Y.-L., Kawamura, K., Cao, F., and Lee, M.: Stable carbon isotopic compositions of low-molecular-weight dicarboxylic acids, oxocarboxylic acids, α-dicarbonyls, and fatty acids: Implications for atmospheric processing of organic aerosols, Journal of Geophysical Research: Atmospheres, 121, 3707-3717, 10.1002/2015jd024081, 2016.

Zhao, W., Kawamura, K., Yue, S., Wei, L., Ren, H., Yan, Y., Kang, M., Li, L., Ren, L., Lai, S., Li, J., Sun, Y., Wang, Z., and Fu, P.: Molecular distribution and compound-specific stable carbon isotopic composition of dicarboxylic acids, oxocarboxylic acids and α-dicarbonyls in PM2.5 from Beijing, China, Atmos. Chem. Phys., 18, 2749-2767, 10.5194/acp-18-2749-2018, 2018.

Zhao, X., Pavuluri, C. M., Dong, Z., Xu, Z., Nirmalkar, J., Jung, J., Fu, P., and Liu, C.-Q.: Molecular Distributions and 13C Isotopic Composition of Dicarboxylic Acids, Oxocarboxylic Acids, and α-dicarbonyls in Wintertime PM2.5 at Three Sites Over Northeast Asia: Implications for Origins and Long-Range Atmospheric Transport, Journal of Geophysical Research: Atmospheres, 128, e2023JD038864, https://doi.org/10.1029/2023JD038864, 2023.